



# *In silico and in vitro* evaluation of nano-enhanced therapeutics for diabetes management

Moumita Sil<sup>1\*</sup>, Debanik Deb<sup>2</sup>, Shauryabrota Dalui<sup>3</sup>, Subhajit Chakraborty<sup>1</sup>, Arunava Goswami<sup>1\*</sup>, Igor Polikarpov<sup>4</sup>

<sup>1</sup>Biological Sciences Division, Indian Statistical Institute, Kolkata, India.

<sup>2</sup>School of Biology, Indian Institute of Science Education and Research, Thiruvananthapuram, India.

<sup>3</sup>Department of Zoology, University of Calcutta, Ballygunge Science College Campus, Kolkata, India.

<sup>4</sup>Department of Biophysics, Institute of Physics in Sao Carlos (IFSC), University of Sao Paulo (USP), São Paulo, Brazil.

## ARTICLE HISTORY

Received on: 06/02/2025  
Accepted on: 18/03/2025  
Available Online: 05/06/2025

### Key words:

Nano-medicine, diabetes, docking, carbohydrate metabolism, silver nanoparticle.

## ABSTRACT

Diabetes mellitus remains a major global health challenge, necessitating safer and more effective therapeutic strategies. Nanotechnology enhances the bioactivity of phytochemicals, offering a novel approach to diabetes management. This study synthesized eco-friendly silver nanoparticles (AgNPs) using phytochemicals from homeopathic mother tinctures (*Strychnos nux-vomica*, *Arnica montana*, and *Atropa belladonna*) and Ayurvedic powders (*Withania somnifera*, *Emblica officinalis*, and *Terminalia chebula*). Characterization via dynamic light scattering (DLS) and electron microscopy field emission scanning electron microscopy, field emission gun transmission electron microscopy confirmed the formation of uniformly spherical AgNPs (10–30 nm), ensuring stability and dispersion. Molecular docking studies assessed the binding affinity of silver atoms with  $\alpha$ -amylase and  $\alpha$ -glucosidase, revealing inhibition via metal chelation. While atomic silver exhibited weak inhibition, AgNPs demonstrated significantly enhanced suppression of enzymatic activity due to their multivalent interactions. Among the formulations, *Emblica officinalis*-derived AgNPs exhibited the most potent inhibition, with  $IC_{50}$  values of 17.5  $\mu$ g/ml ( $\alpha$ -amylase) and 12.87  $\mu$ g/ml ( $\alpha$ -glucosidase), surpassing acarbose. Their efficacy was further linked to oxidative stress induction, influencing glucose metabolism and enzyme inhibition. The cytotoxicity of *E. officinalis*-derived AgNPs was assessed using the MTT assay on MDA-MB-231 cells. A concentration-dependent cellular response indicated active nanoparticle uptake, suggesting interactions with intracellular signaling pathways. The biointeractive potential of these nanoparticles further supports their role as therapeutic agents. This study highlights the potential of phytochemically synthesized AgNPs as effective antidiabetic agents. The integration of nanotechnology with traditional medicine offers a sustainable therapeutic approach. Further research into pharmacokinetics, *in vivo* efficacy, and mechanistic pathways will be crucial for clinical translation.

## INTRODUCTION

Diabetes mellitus is a significant global health challenge [1–4]. The prevalence of diabetes has surged dramatically, with an estimated 828 million adults aged 18 years and older affected in 2022, compared to 630 million in

1990 [5]. This chronic disease imposes substantial morbidity and mortality worldwide [6,7]. Addressing this burden necessitates the development of effective and safe therapeutic interventions. Targeting the inhibition of  $\alpha$ -amylase and  $\alpha$ -glucosidase enzymes to reduce glucose absorption has emerged as a crucial strategy [8–10]. However, existing drugs, such as the FDA-approved enzyme inhibitor acarbose, are associated with considerable side effects [11–13]. Traditional medicinal systems, particularly in Asian and African countries, have long utilized natural compounds for therapeutic purposes [14–16]. Phytochemicals—bioactive compounds produced by

\*Corresponding Author  
Moumita Sil and Arunava Goswami, Biological Sciences Division,  
Indian Statistical Institute, Kolkata, India. E-mails: moumitasil20@  
gmail.com and agoswami@isical.ac.in

plants through secondary metabolism—are diverse and include flavonoids, alkaloids, polysaccharides, amino acids, proteins, enzymes, vitamins, phenolic acids, tannins, saponins, and terpenoids [17]. These compounds exhibit various medicinal properties, finding applications in pharmaceuticals [18] and as antimicrobial agents [19]. Phytochemicals derived from fruits and vegetables play a critical role in preventing chronic diseases by modulating metabolic processes [20]. Notably, flavonoids have demonstrated synergistic inhibitory effects on  $\alpha$ -amylase and  $\alpha$ -glucosidase, making them promising candidates for antidiabetic applications [21]. Beyond their therapeutic potential, flavonoids are also employed in aquaculture as growth promoters and immunostimulants [22,23]. Nanotechnology offers a novel avenue for enhancing the bioactivity and efficacy of phytochemicals. Nanoparticles, defined as colloidal particles with diameters under 100 nm, possess unique physical, chemical, and biological properties due to their high surface area-to-volume ratio [24–27]. These properties make them valuable tools in biomedicine and therapeutic development. However, conventional nanoparticle synthesis methods often involve expensive energy inputs and toxic chemicals, resulting in hazardous waste [28,29]. In contrast, green synthesis approaches utilize biological sources such as plants, fungi, algae, and bacteria, offering a sustainable and eco-friendly alternative [30,31]. Phytochemicals facilitate the reduction of precursor salts and the stabilization of nanoparticles through complex redox processes.

This study focuses on the biosynthesis of silver nanoparticles (AgNPs) using virgin mother tinctures (*Strychnos nux-vomica*, *Arnica montana*, and *Atropa belladonna*) and Ayurvedic powders (*Withania somnifera*, *Embllica officinalis*, and *Terminalia chebula*) as natural reducing agents. The integration of nanotechnology with traditional medicinal systems provides a promising strategy for developing accessible and cost-effective nanomedicines, particularly for underserved populations. The biosynthesized AgNPs were characterized using dynamic light scattering (DLS), field emission scanning electron microscopy (FESEM), and field emission gun transmission electron microscopy (FEG-TEM), revealing uniform dispersion, spherical morphology, and particle sizes between 10 and 30 nm.

We performed molecular docking simulations to evaluate the binding affinity of Silver (Ag) towards  $\alpha$ -amylase and  $\alpha$ -glucosidase using AutoDock Vina. Custom parameters were incorporated to enable accurate docking calculations, and interaction analyses were conducted using PyMOL. The results indicated that Silver exhibited a weak theoretical inhibition potential against  $\alpha$ -amylase (binding energy:  $-1.3$  kcal/mol,  $K_i$ : 111.31 mM) and a relatively stronger inhibition against  $\alpha$ -glucosidase (binding energy:  $-1.4$  kcal/mol,  $K_i$ : 94.01 mM). The interaction analyses revealed electrostatic and Van der Waals forces with key amino acid residues. The *in silico* studies led us to perform *in vitro* studies for evaluating the antidiabetic potential of silver nanoparticles to inhibit key starch-digesting enzymes,  $\alpha$ -amylase, and  $\alpha$ -glucosidase. Results demonstrated superior enzyme inhibition compared to acarbose, suggesting that AgNPs synthesized through phytochemical-mediated processes may effectively

reduce hyperglycemia. This positions them as promising candidates for diabetes management. The cytotoxicity of *Embllica officinalis*-derived AgNPs, evaluated via the MTT assay on MDA-MB-231 cells, showed a concentration-dependent response, indicating active nanoparticle uptake and potential intracellular interactions, reinforcing their therapeutic relevance. In contrast to traditional nanoparticle synthesis methods, this green approach harnesses bioactive phytochemicals from mother tinctures and Ayurvedic powders, offering an eco-friendly and biocompatible alternative. These findings highlight the potential of integrating nanotechnology with traditional medicine systems to develop innovative, affordable, and sustainable healthcare solutions.

## MATERIALS AND METHOD

### Materials

All chemicals were procured from Sigma Aldrich, while glassware and plasticware were sourced from Tarsons and Borosil unless otherwise specified.

### Methods

#### Synthesis of Nanoparticles

Virgin mother tinctures (*S. nux-vomica*, *A. montana*, and *A. belladonna*) were sourced from Schwab Inc., Germany, while Ayurvedic powders (*W. somnifera*, *Embllica officinalis*, and *T. chebula*) were obtained from M/S Dabur Inc., India. AgNPs were synthesized using silver nitrate (AgNO<sub>3</sub>) as a precursor and the aforementioned tinctures and powders as natural reducing agents. Specific quantities of AgNO<sub>3</sub> were added: 68 mg for *A. montana* and *A. belladonna*, 100 mg for *S. nux-vomica*, and 20 mg for each Ayurvedic powder. The mixtures were stirred under controlled conditions—800 rpm at 80°C for 2 hours for *A. belladonna* and *W. somnifera*, 30 minutes for *S. nux-vomica*, *E. officinalis*, and *T. chebula*, and 24 hours at 45°C for *A. montana*. The formation of nanoparticles was indicated by a color change in the mixtures. Nanoparticles were stabilized using PEG-400 and phosphate buffer (5:1) with stirring (1,300 rpm, 45 minutes), followed by diluted formic acid addition and further stirring (15 minutes). The solution was centrifuged (7,000 rpm, 20 minutes, 25°C), and precipitates were washed thrice with 99% ethanol, and centrifuged for 20, 20, and 10 minutes. The final precipitates were dried in a laminar flow hood and subjected to further physicochemical and biological characterization.

#### Characterization of synthesized biogenic AgNPs

We have utilized TEM, Scanning Electron Microscopy (SEM), and DLS for a comprehensive characterization of our samples, offering essential insights into their morphology, size distribution, and surface properties—key aspects relevant to our study.

#### Particle size analysis

Dynamic light scattering was employed to determine the particle size distribution and colloidal stability of the synthesized nanoparticles. This technique provides the

Z-average size and polydispersity index (PDI) as key parameters. For analysis, nanoparticles were suspended in ethanol (Merck) and subjected to ultrasonic treatment for 40 minutes using an ultra-bath sonicator to achieve homogenous dispersion. After sonication, the hydrodynamic diameter (Z-average) and PDI of the nanoparticle suspensions were measured using a MALVERN Zetasizer (UK).

#### *Transmission electron microscopy and Scanning electron microscopy*

Field Emission Gun Transmission Electron Microscopy (JEM-2100F, JEOL Ltd., Japan) and FESEM were utilized to investigate the physicochemical properties of the synthesized nanoparticles. Field emission Gun Transmission Electron Microscopy provided detailed information on the morphology, size, and shape of the nanoparticles. For TEM analysis, a drop of diluted nanoparticle solution was placed onto a carbon-coated copper grid and allowed to dry for 48 hours. SEM was performed by drop-casting a diluted nanoparticle solution onto a silicon wafer.

#### **Docking and validation of silver-mediated enzyme inhibition**

To assess the binding affinity of a small-molecule ligand, Ag, towards  $\alpha$ -amylase and  $\alpha$ -glucosidase, molecular docking simulations were performed using AutoDock Vina 1.5.7. The three-dimensional (3D) molecular structure of Silver was generated using Avogadro and saved in silver.pdb format. Since AutoDock does not inherently support Ag as a ligand, custom parameters were incorporated by modifying the AD4.1\_bound.dat and AD4\_parameters.dat files to enable accurate docking calculations. The 3D crystallographic structures of the target enzymes were retrieved from the RCSB Protein Data Bank: human pancreatic  $\alpha$ -amylase (PDB ID: 4GQR) and  $\alpha$ -glucosidase (PDB ID: 5NN8). The docking interactions between Silver and the target enzymes were analyzed, and the results were visualized using PyMOL software to evaluate binding modes and potential interactions with various amino acids side chains of the docked protein. To determine the inhibition constant ( $K_i$ ) from molecular docking results, we utilized a computational approach based on the relationship between the Gibbs free energy of binding ( $\Delta G$ ) and the equilibrium dissociation constant. The calculation was performed using Python (version 3.10), executed within the Spyder IDE, which is part of the Anaconda distribution. The script employs the math module for numerical computation.

#### Computational approach

The inhibition constant was calculated using the equation:

$$K_i = e^{\frac{\Delta G}{RT}}$$

where:

$K_i$  is the inhibition constant in molar (M),  $\Delta G$  (binding free energy) is given in kcal/mol,

R is the universal gas constant ( $1.987 \times 10^{-3}$  kcal/(mol·K)),

T is the absolute temperature (298 K, representing physiological conditions).

The math.exp () function in Python was used to compute the exponential term. The final values of  $K_i$  were converted into millimolar (mM) units for better interpretation.

#### **In-vitro enzymatic inhibition assays**

##### *Alpha amylase inhibition assay*

For the alpha-amylase inhibition assay, a 100  $\mu$ l aliquot of the substrate (1% soluble starch in a 20 mM sodium phosphate buffer containing 6.7 M sodium chloride, pH 6.9) was mixed with 50  $\mu$ l of the nanoparticle solution and incubated at 37°C for 10–15 minutes. Next, 100  $\mu$ l of alpha amylase (A8220, Sigma Aldrich) at a concentration of 2 U/ml was added, followed by an additional 30-minute incubation. Afterward, 100  $\mu$ l of the mixture was withdrawn, and 50  $\mu$ l of Di-nitro-salicylic acid (DNSA) solution was added, which was then heated at 82°C for 30 minutes. Absorbance was measured at 540 nm. The DNSA solution was prepared by dissolving 96 mM DNSA in 10 ml of a 5.3 M sodium potassium tartrate solution in 2 M sodium hydroxide, with acarbose (A8980, Sigma Aldrich) serving as a standard.

##### *Alpha-glucosidase inhibition assay*

The activity of  $\alpha$ -glucosidase was evaluated in a 100 mM sodium phosphate buffer at pH 6.8. The reaction mixture contained 0.1 U/ml of the enzyme (G5003, Sigma Aldrich) and 1.25 mM 4-nitrophenyl  $\alpha$ -D-glucopyranoside (N1377, Sigma Aldrich), with or without nanoparticles, in a total volume of 200  $\mu$ l, incubated at 37°C. Acarbose (A8980, Sigma Aldrich) was used as the standard for comparison.

##### **Cytotoxicity study**

The cytotoxicity of synthesized AgNPs was assessed using the MTT assay. MDA-MB-231 cells were cultured in DMEM with 10% FBS and 1% antibiotic–antimycotic solution at 37°C, 5% CO<sub>2</sub> for 24 hours before treatment. The cells were then exposed to AgNPs (2.5–80  $\mu$ g/ml) in a 96-well plate for 24 hours. To assess cytotoxicity, MTT solution (0.1 mg/ml) was added and incubated for 4 hours at 37°C, 5% CO<sub>2</sub>. Metabolically active cells reduced MTT to insoluble purple formazan, which was solubilized and quantified at 570 nm. Cell viability was calculated and compared to the control group.

##### **Statistical analysis**

Statistical significance across experimental conditions was evaluated using one-way ANOVA in GraphPad Prism (version 8.4.3).

## **RESULTS AND DISCUSSION**

### **Characterization of biogenically synthesized nano-silver**

Dynamic light scattering analysis revealed hydrodynamic sizes of 141.4 nm for *A. montana*-derived AgNPs, 312.7 nm for *A. belladonna*-derived AgNPs, and 124

nm for *S. nux-vomica*-derived AgNPs. The hydrodynamic radii for *W. somnifera*-derived AgNP were

123.6 nm, for *E. officinalis*-derived AgNP was 130.2 nm, and for AgNP from *Terminalia chebula* was 131.6 nm. The PDI values were 0.232 for *A. montana*, 0.350 for *Atropa belladonna*, and 0.225 for *S. nux-vomica*-based AgNPs, PDI values for AgNPs derived from *W. somnifera*, *E. officinalis*, and *T. chebula* were 0.238, 0.211, and 0.252, respectively, indicating that all synthesized nanoparticle systems exhibit polydispersity, with *A. belladonna*-derived AgNPs showing the highest degree of size distribution variability. The PDI values of silver nanoparticles derived from both Ayurvedic mixture and virgin Homeopathic mother tinctures indicate potential stability (Fig. 1). Previous studies suggest that PDI values below 0.3 indicate homogeneous dispersion, while higher values correspond to heterogeneous nanoparticles with variable sizes [32].

The morphology, size, and structural details of the synthesized AgNPs were further examined using FEG-TEM. TEM images revealed that the AgNPs predominantly exhibited a spherical shape, with particle sizes ranging between 5 and 100 nm. This size estimate obtained from TEM analysis was notably smaller than the hydrodynamic sizes measured by DLS, likely due to the absence of solvent-related effects in TEM measurements (Figs. 2 and 3).

FESEM images provided clear evidence of the formation of silver nanoparticles, showing a uniform distribution of nanoparticles with predominantly spherical morphology. Additionally, the presence of polyethylene glycol (PEG-400) coating on the surface of the AgNPs

was confirmed by the FESEM images, which indicated the stabilizing effect of PEG-400 on the nanoparticles (Figs. 2 and 3). The microscopic studies also confirmed the uniformity in size and shape of the AgNPs as obtained from the Ayurvedic mixtures.

### In-silico studies

Molecular docking studies were conducted to evaluate the binding interactions of Ag with human pancreatic  $\alpha$ -amylase (PDB ID: 4GQR). The docking analysis revealed that the binding affinity energy was consistent across docking modes 1, 2, 3, and 4 (Table 1). However, docking validation criteria require that a root mean square deviation (RMSD) of  $\leq 2$  Å be maintained to ensure a reliable binding pose [33]. Among the obtained docking modes, only mode 1 satisfied this criterion, making it the most appropriate pose for further analysis. For mode 1, the calculated binding energy was  $-1.3$  kcal/mol, and the inhibition constant ( $K_i$ ) was 111.31 mM, indicating a weak theoretical inhibition potential of Silver towards  $\alpha$ -amylase [34,35]. The interaction analysis revealed that the Silver atom participated in binding through non-covalent interactions with three key amino acid residues: THR254 with bond distances of 2.5 Å and 2.4 Å, GLN232 at 3.4 Å, and VAL234 at 2.4 Å (Fig. 4). These interactions suggest that Silver engages with  $\alpha$ -amylase through weak electrostatic or Van der Waals forces rather than strong hydrogen bonding or covalent interactions.

For  $\alpha$ -glucosidase (PDB ID: 5NN8), mode 1 exhibited the highest binding affinity energy and the lowest RMSD, making it the most reliable docking pose (Table 2). Other docking

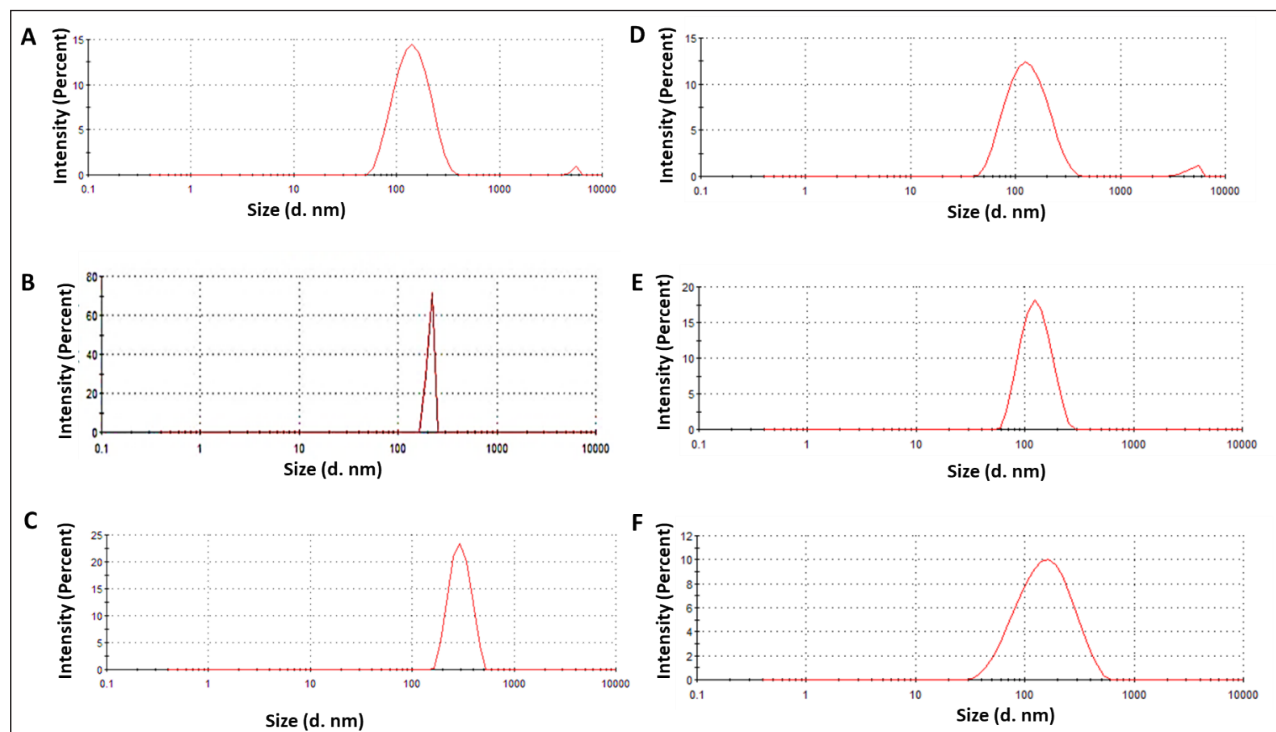


**Figure 1.** A, B, C—DLS of nanoparticles as obtained from *A. montana*, *S. nux-vomica*, and *A. belladonna*. D, E, F—DLS of nanoparticles as obtained from *W. somnifera*, *Emblica officinalis*, and *T. chebula*.

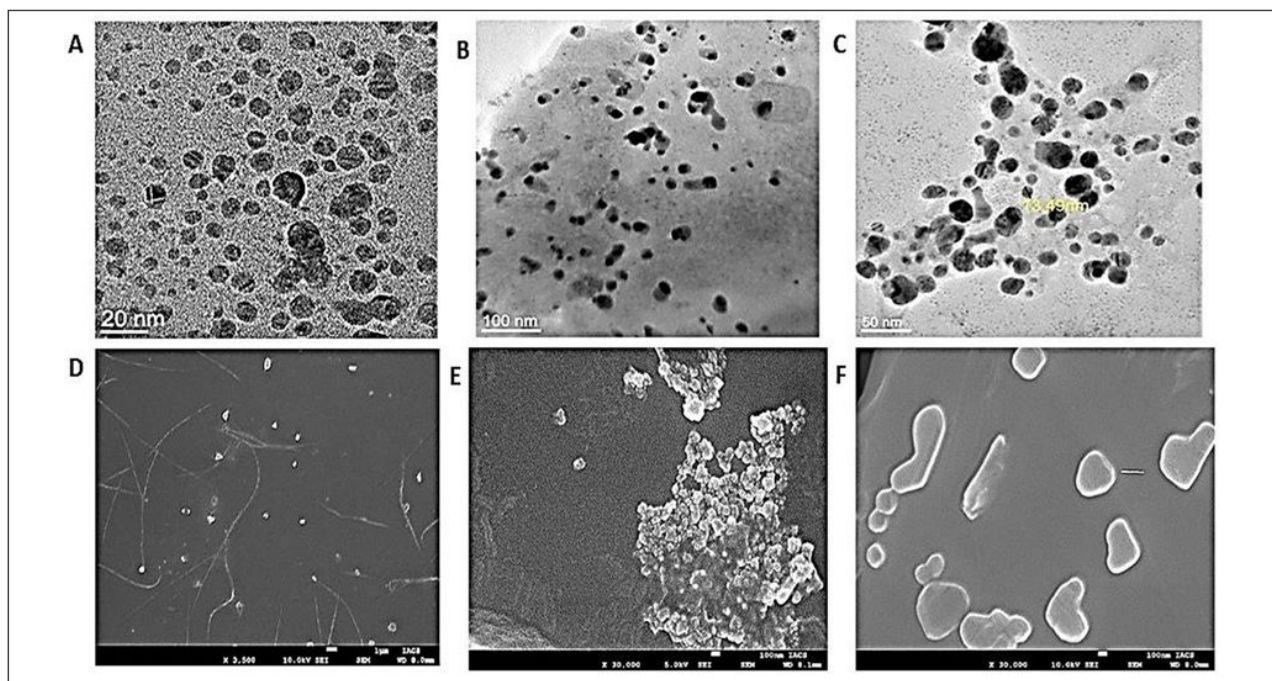


**Figure 2.** A, B, C—Transmission Electron Microscope (JEM-2100F, JEOL Ltd., Japan) image of AgNPs from *A. montana*, *S. nux-vomica*, and *A. belladonna*. D, E, F—Scanning Electron Microscopy (FEI Quanta 250 FEG-SEM) image of AgNPs from *Arnica montana*, *S. nux-vomica*, and *A. belladonna*.

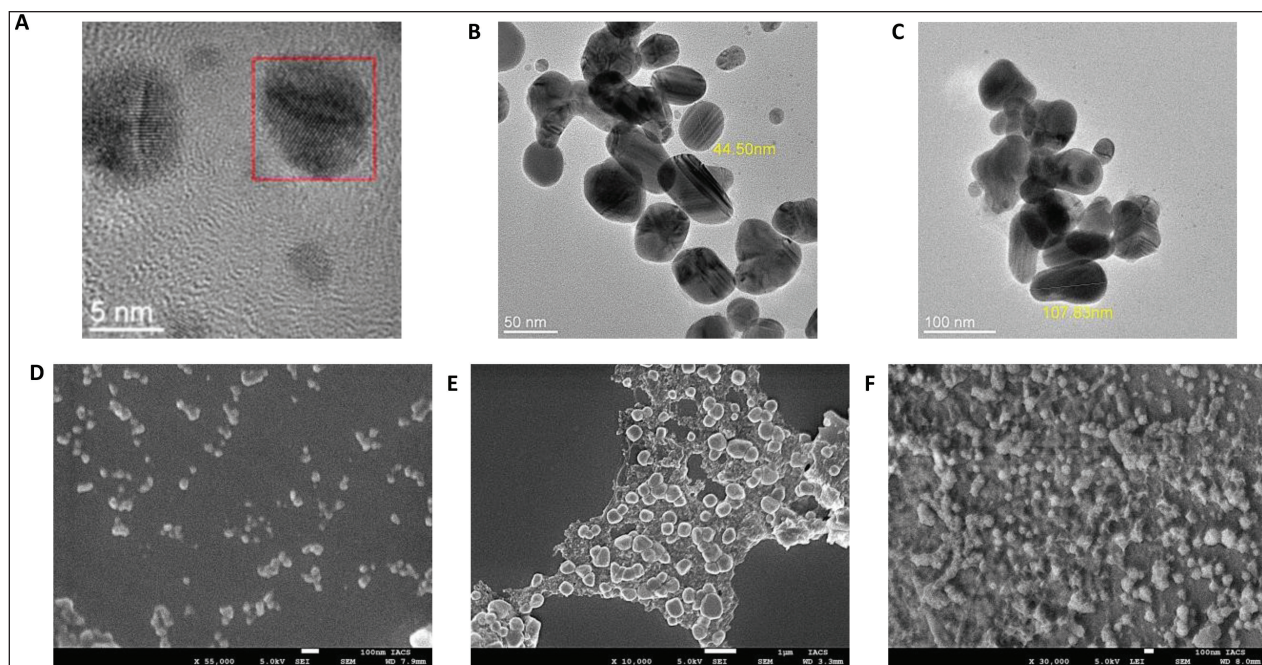


**Figure 3.** A, B, C—Transmission Electron Microscope (JEM-2100F, JEOL Ltd., Japan) image of AgNPs from *W. somnifera*, *E. officinalis*, and *T. chebula*. D, E, F—Scanning Electron Microscopy (FEI Quanta 250 FEG-SEM) image of AgNPs from *Withania somnifera*, *E. officinalis*, and *T. chebula*.

modes, including modes 2, 3, 4, and 5, demonstrated favorable binding energies but were rendered invalid due to RMSD values exceeding 2 Å. Notably, mode 9 had a binding energy of  $-1.2$  kcal/mol, but the RMSD exceeded the acceptable threshold, disqualifying it as a valid binding pose. For mode 1, the binding

energy was  $-1.4$  kcal/mol, and the  $K_i$  was 94.01 mM, which was lower than that observed for  $\alpha$ -amylase. This lower  $K_i$  value suggests that Silver exhibits a higher inhibitory potential towards  $\alpha$ -glucosidase than  $\alpha$ -amylase. This suggests that Silver has a relatively higher affinity for  $\alpha$ -glucosidase. Interaction analysis

of the selected pose (mode 1) indicated that Silver participated in metal chelation interactions with five amino acid residues: PHE649 at 2.6 Å, GLY648 at 3.3 Å, LEU650 at 2.6 Å, GLY651 at 2.4 Å, and SER619 at 2.0 Å (Fig. 4).

The docking algorithm employed in this study accounted for multiple energetic contributions, including final intermolecular energy, Van der Waals interactions, hydrogen bond energy, electrostatic energy, and roto-translational energy.

**Table 1.** Generated log file for silver and alpha-amylase interaction.

Mode	Affinity	Distance from best mode	
	kcal/mol	RMSD l.b.	RMSD u.b.
1	-1.3	0.000	0.000
2	-1.3	16.308	16.308
3	-1.3	15.733	15.733
4	-1.3	18.956	18.956
5	-1.3	30.256	30.256
6	-1.2	23.285	23.285
7	-1.2	32.386	32.386
8	-1.2	21.204	21.204
9	-1.2	15.709	15.709

Since silver is a single atom, torsional energy contributions were considered negligible. Unlike conventional small-molecule inhibitors that rely on multiple rotatable bonds to optimize their fit within the active site, silver's inhibitory effects are likely mediated through metal coordination and weak electrostatic interactions.

While the binding energy of a single silver atom may appear lower compared to potent commercially available inhibitors, it is critical to consider the potential enhancement of inhibitory effects when silver is utilized in nanoparticle form AgNPs. Given that nanoparticles consist of multiple silver atoms, their cumulative binding affinity is expected to be significantly greater than that of an individual silver atom. AgNPs exhibit a high surface area-to-volume ratio, enabling multivalent interactions with catalytic and allosteric sites of  $\alpha$ -amylase and  $\alpha$ -glucosidase, thereby enhancing inhibition. Their unique physicochemical properties, including localized surface plasmon resonance and increased charge density, facilitate stronger electrostatic interactions and metal coordination with key enzymatic residues. Additionally, phytochemicals adsorbed during green synthesis contribute to enzyme binding through synergistic interactions, further augmenting the inhibitory potential of AgNPs beyond atomic

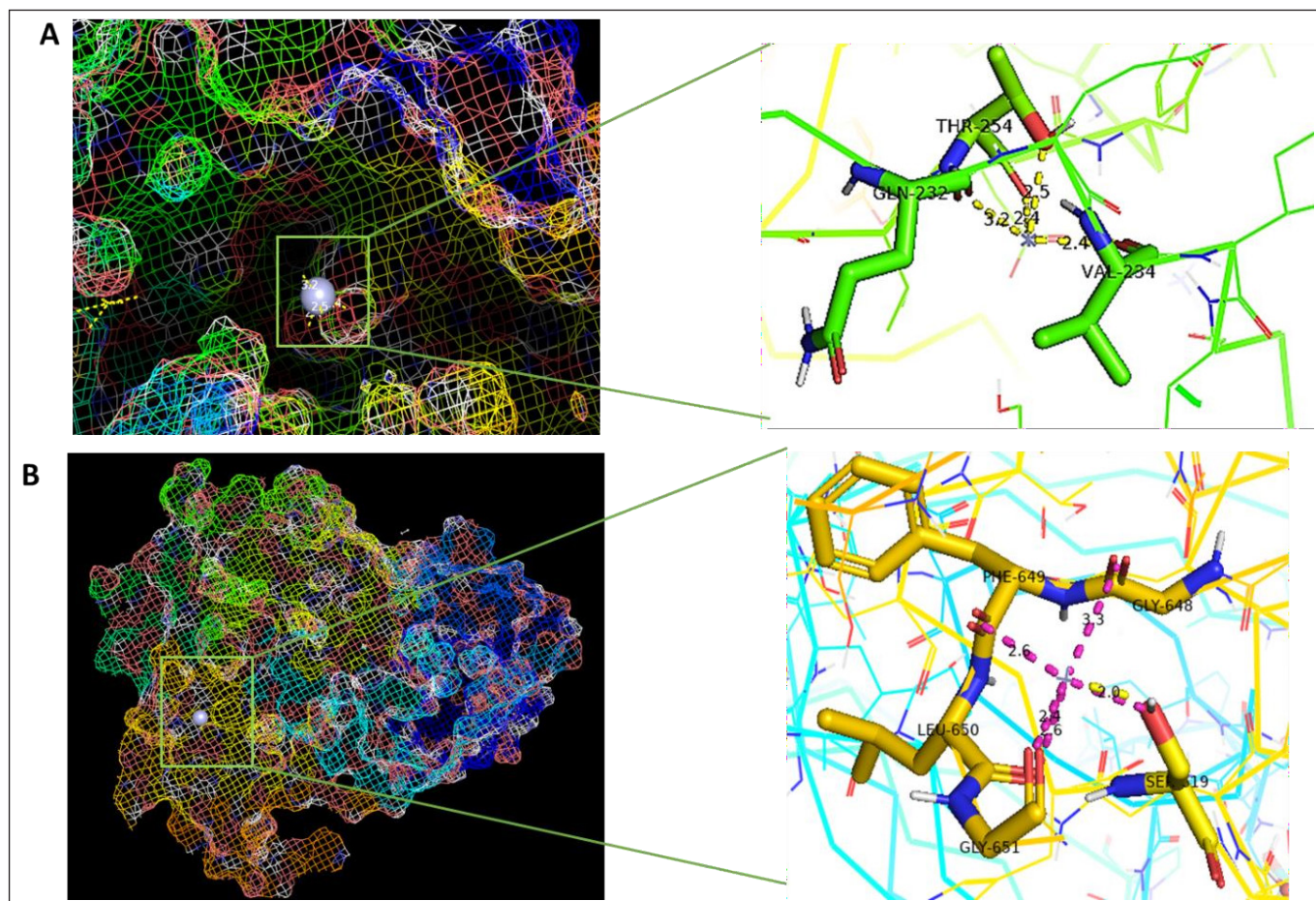


**Figure 4.** Molecular docking and interactions between silver atom and amino acids (A) alpha amylase and (B) alpha glucosidase.

silver. This suggests that AgNPs may exert a more pronounced inhibitory effect on carbohydrate-hydrolyzing enzymes [36].

From these results, it can be inferred that silver demonstrates inhibitory activity against both  $\alpha$ -amylase and  $\alpha$ -glucosidase, with a stronger theoretical inhibition towards  $\alpha$ -glucosidase. This finding supports the potential application of silver-based compounds in modulating carbohydrate metabolism, potentially contributing to the development of novel therapeutics for conditions such as diabetes and metabolic disorders.

### In vitro anti-diabetic assay using biogenically synthesized AgNPs

The inhibitory effects of AgNPs on  $\alpha$ -amylase and  $\alpha$ -glucosidase activities were evaluated, and the resulting IC<sub>50</sub> values were compared with that of the commercially available  $\alpha$ -amylase and  $\alpha$ -glucosidase inhibitor, Acarbose. Acarbose demonstrated IC<sub>50</sub> values of 1023.784  $\mu$ g/ml for  $\alpha$ -amylase and 2532.417  $\mu$ g/ml for  $\alpha$ -glucosidase. In contrast, AgNPs

synthesized from various medicinal plants exhibited varying degrees of enzyme inhibition.

AgNPs from *A. montana* exhibited IC<sub>50</sub> values of 128.65  $\mu$ g/ml for  $\alpha$ -amylase and 1662.02  $\mu$ g/ml for  $\alpha$ -glucosidase, while AgNPs from *A. belladonna* demonstrated IC<sub>50</sub> values of 228.31  $\mu$ g/ml for  $\alpha$ -amylase and 339.414  $\mu$ g/ml for  $\alpha$ -glucosidase. AgNPs synthesized from *Strychnos nux-vomica* showed IC<sub>50</sub> values of 230.122  $\mu$ g/ml for  $\alpha$ -amylase and 98.47  $\mu$ g/ml for  $\alpha$ -glucosidase, demonstrating considerable efficacy in inhibiting both enzymes.

AgNPs derived from *W. somnifera* showed moderate inhibitory effects, with IC<sub>50</sub> values of 131.396  $\mu$ g/ml for  $\alpha$ -amylase and 339.2  $\mu$ g/ml for  $\alpha$ -glucosidase. AgNPs synthesized from *Embllica officinalis* exhibited the most potent enzyme inhibition, with IC<sub>50</sub> values of 17.5  $\mu$ g/ml for  $\alpha$ -amylase and 12.87  $\mu$ g/ml for  $\alpha$ -glucosidase, significantly outperforming Acarbose and other plant-derived AgNPs. *Terminalia chebula*-derived AgNPs showed IC<sub>50</sub> values of 319.559  $\mu$ g/ml for  $\alpha$ -amylase and 226.67  $\mu$ g/ml for  $\alpha$ -glucosidase, indicating

**Table 2.** Generated log file for silver and alpha-glucosidase interaction.

Mode	Affinity	Distance from best mode	
	kcal/mol	RMSD l.b.	RMSD u.b.
1	-1.4	0.000	0.000
2	-1.3	23.371	23.371
3	-1.3	10.046	10.046
4	-1.3	48.438	48.438
5	-1.3	24.234	24.234
6	-1.2	43.264	43.264
7	-1.2	14.987	14.987
8	-1.2	36.639	36.639
9	-1.2	3.963	3.963

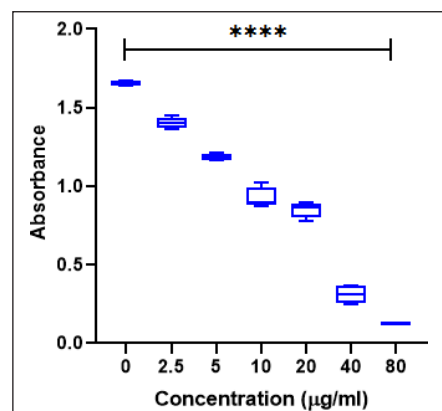


**Figure 6.** Cytotoxicity assay of AgNP on MDA-MB-231 cell line. \*\*\*\* $p \leq 0.0001$ .

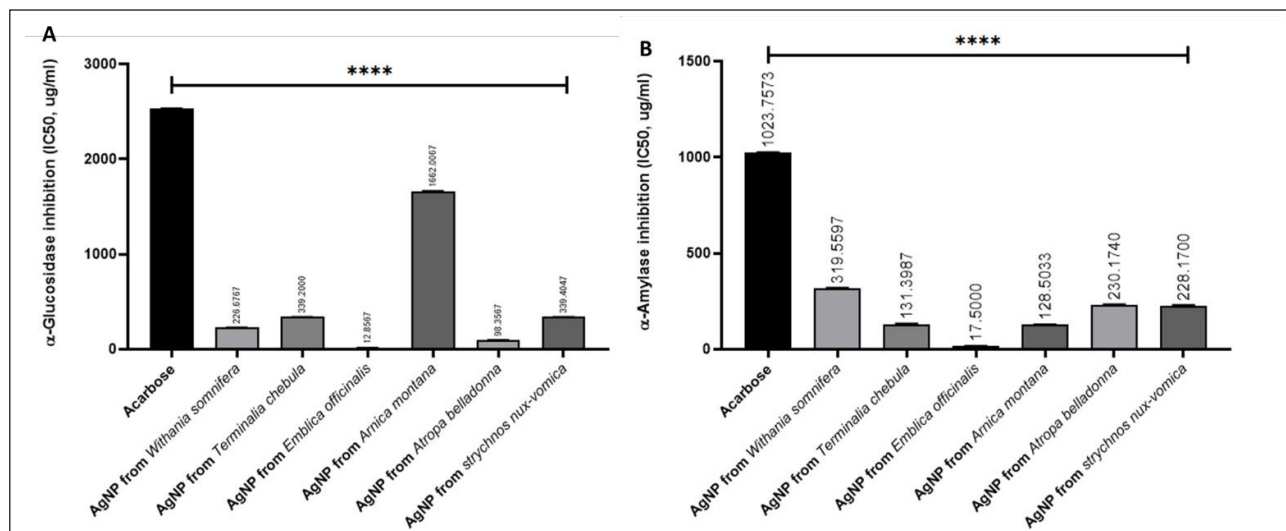


**Figure 5.** Starch enzyme inhibition assay; (A) alpha amylase and (B) alpha glucosidase with synthesized silver nanoparticles from six sources and Acarbose as standard. \*\*\*\* $p \leq 0.0001$ . Software: GraphPad Prism 8.4.3.

moderate inhibitory activity compared to other formulations (Fig. 5).

#### **In vitro cytotoxicity study**

The cytotoxic effects of *E. officinalis* derived AgNPs on MDA-MB-231 cells were assessed using the MTT assay because this nanoparticle outperformed as an anti-diabetic agent in comparison to the rest. A concentration-dependent decline in cell viability was observed, as indicated by the progressive decrease in absorbance at 570 nm (Fig. 6). AgNP exposure at concentrations ranging from 2.5 to 80 µg/ml resulted in a significant decline in metabolic activity ( $p < 0.0001$ ). At a 20 µg/ml dose, absorbance was reduced to approximately half of the control group, while the highest concentration (80 µg/ml) exhibited minimal absorbance, indicating near-complete cytotoxicity. These findings highlight the potent inhibitory effect of AgNPs on MDA-MB-231 cell proliferation in a dose-dependent manner.

#### **CONCLUSION**

This study provides a comprehensive comparison between *in silico* and *in vitro* approaches in evaluating the antidiabetic potential of AgNPs synthesized using phytochemical-rich homeopathic mother tinctures and Ayurvedic mixtures. Molecular docking experiments demonstrated that silver exhibited weak inhibitory potential against  $\alpha$ -amylase (binding energy:  $-1.3$  kcal/mol,  $K_i$ : 111.31 mM) and relatively stronger inhibition against  $\alpha$ -glucosidase (binding energy:  $-1.4$  kcal/mol,  $K_i$ : 94.01 mM). These findings suggested that silver engages in electrostatic and Van der Waals interactions with target enzymes, necessitating further validation through *in vitro* enzyme inhibition assays.

*In vitro* studies confirmed that AgNPs synthesized using traditional medicinal plant extracts significantly enhanced enzyme inhibition. AgNPs derived from *E. officinalis* demonstrated the highest inhibitory activity, with  $IC_{50}$  values of 17.5 µg/ml for  $\alpha$ -amylase and 12.87 µg/ml for  $\alpha$ -glucosidase, outperforming the commercial inhibitor acarbose. Acarbose acts as an antidiabetic agent by inhibiting both the enzymes  $\alpha$ -amylase and  $\alpha$ -glucosidase. This aligns with the docking predictions, where silver displayed a higher affinity towards  $\alpha$ -glucosidase, reinforcing the potential of phytochemical-assisted AgNP synthesis in enzyme inhibition.

Similarly, another study synthesized AgNPs using *Allium sativum* (garlic) extract and assessed their antidiabetic properties through *in vitro* and *in silico* studies. Their results demonstrated that the garlic-derived AgNPs effectively inhibited  $\alpha$ -amylase and  $\alpha$ -glucosidase activities, enhanced glucose uptake in L-6 myotubes, reduced hepatic glucose production in HepG2 cells, and interacted with key amino acid residues of the target enzymes in molecular docking analyses [36]. A comparative analysis of AgNP synthesis from homeopathic and Ayurvedic sources revealed distinct stability and efficacy profiles. Among the synthesized nanoparticles, *Emblica officinalis*-derived AgNPs emerged as the most effective, exhibiting superior inhibition of both  $\alpha$ -amylase and  $\alpha$ -glucosidase. This enhanced activity can be attributed to the phytochemical composition of

*Emblica officinalis*, which includes high levels of antioxidants such as ellagic acid and gallic acid, known for their metal-chelating and enzyme-inhibitory properties. Additionally, the smaller, more uniform particle size of these AgNPs likely contributed to their higher surface activity and bioavailability, facilitating stronger interactions with target enzymes.

The enhanced inhibitory potential of AgNPs can be attributed to multiple mechanisms, including metal chelation, which facilitates strong interactions with active site residues of carbohydrate-hydrolyzing enzymes, leading to enzyme inactivation. Additionally, AgNPs are known to induce oxidative stress, which may contribute to altered cellular metabolic processes, further influencing enzyme activity and glucose metabolism. The potential cellular uptake of AgNPs adds another dimension to their bioactivity, as internalized nanoparticles may interact with intracellular signaling pathways involved in glucose regulation.

Furthermore, the cytotoxicity assay using the MTT method on MDA-MB-231 cells demonstrated a concentration-dependent influence of *E. officinalis*-derived AgNPs on metabolic activity. The results indicated an active cellular response to increasing nanoparticle concentrations, reflecting their biointeractive potential.

Overall, this study highlights the efficacy of phytochemically synthesized AgNPs as promising antidiabetic agents. The integration of nanotechnology with traditional medicine offers an innovative, sustainable, and biocompatible approach to diabetes management. Further investigations into the long-term stability, bioavailability, and mechanistic pathways of these nanoparticles will be essential for their translational application in therapeutic settings.

#### **ACKNOWLEDGMENT**

We are thankful to our field assistants, Mr. Ashim Dhar and Mrs. Piyali Maitra, for their contributions to fieldwork and the development and maintenance of laboratory infrastructure.

#### **AUTHOR CONTRIBUTIONS**

All authors made substantial contributions to conception and design, acquisition of data, or analysis and interpretation of data; took part in drafting the article or revising it critically for important intellectual content; agreed to submit to the current journal; gave final approval of the version to be published; and agree to be accountable for all aspects of the work. All the authors are eligible to be an author as per the International Committee of Medical Journal Editors (ICMJE) requirements/guidelines.

#### **FINANCIAL SUPPORT**

There is no funding to report.

#### **CONFLICT OF INTEREST**

The authors report no financial or any other conflicts of interest in this work.

#### **ETHICAL APPROVALS**

This study does not involve experiments on animals or human subjects.

## DATA AVAILABILITY

All data generated and analyzed are included in this research article.

## PUBLISHER'S NOTE

All claims expressed in this article are solely those of the authors and do not necessarily represent those of the publisher, the editors and the reviewers. This journal remains neutral with regard to jurisdictional claims in published institutional affiliation.

## USE OF ARTIFICIAL INTELLIGENCE (AI)-ASSISTED TECHNOLOGY

The authors declares that they have not used artificial intelligence (AI)-tools for writing and editing of the manuscript, and no images were manipulated using AI.

## REFERENCES

- Wild S, Roglic G, Green A, Sicree R, King H. Global prevalence of diabetes: estimates for the year 2000 and projections for 2030. *Diabetes Care*. 2004;27(5):1047–53.
- Sharma R, Juyal D, Negi A. Epidemiology of diabetes mellitus and its recent awareness with the use of advance medication. *Pharma Innov J*. 2018;7(6):87.
- Vargas-Uricoechea H, Casas-Figueroa LÁ. Epidemiología de la diabetes mellitus en Sudamérica: la experiencia de Colombia. *Clín Investig Arterioscler*. 2016;28(5):245–56.
- Zhou B, Rayner AW, Gregg EW, Sheffer KE, Carrillo-Larco RM, Bennett JE, *et al.* Worldwide trends in diabetes prevalence and treatment from 1990 to 2022: a pooled analysis of 1108 population-representative studies with 141 million participants. *Lancet*. 2024;404(10467):2077–93.
- Wahidin M, Achadi A, Besral B, Kosen S, Nadjib M, Nurwahyuni A, *et al.* Projection of diabetes morbidity and mortality till 2045 in Indonesia based on risk factors and NCD prevention and control programs. *Sci Rep*. 2024;14(1):5424.
- Yameny AA. Diabetes mellitus overview 2024. *J Biosci Appl Res*. 2024;10(3):641–5.
- Ndarawit W, Ochieng CO, Angwenyi D, Cruz JN, Santos CB, Kimani NM. Discovery of  $\alpha$ -amylase and  $\alpha$ -glucosidase dual inhibitors from NPASS database for management of Type 2 Diabetes Mellitus: a chemoinformatic approach. *PLoS One*. 2024;19(11):e0313758.
- Li X, Bai Y, Jin Z, Svensson B. Food-derived non-phenolic  $\alpha$ -amylase and  $\alpha$ -glucosidase inhibitors for controlling starch digestion rate and guiding diabetes-friendly recipes. *Lwt*. 2022;153:112455.
- Shrestha D, Sharma P, Adhikari A, Mandal AK, Verma A. A review on Nepalese medicinal plants used traditionally as alpha-amylase and alpha-glucosidase inhibitors against diabetes mellitus. *Curr Tradit Med*. 2021;7(5):63–72.
- Khan F, Khan MV, Kumar A, Akhtar S. Recent advances in the development of alpha-glucosidase and alpha-amylase inhibitors in type 2 diabetes management: insights from *in silico* to *in vitro* studies. *Curr Drug Targets*. 2024;25(12):782–95.
- Dong Y, Sui L, Yang F, Ren X, Xing Y, Xiu Z. Reducing the intestinal side effects of acarbose by baicalein through the regulation of gut microbiota: an *in vitro* study. *Food Chem*. 2022;394:133561.
- Fisher M. Acarbose and alpha glucosidase inhibitors. *Diabetes Drug Notes*. 2022;27:229–38.
- Che CT, George V, Ijiru TP, Pushpangadan P, Andrae-Marobela K. Traditional medicine. In: Badal S, Delgoda R, editors. *Pharmacognosy*. Cambridge, MA: Academic Press; 2024. pp. 11–28.
- Adeleye OA, Femi-Oyewo MN, Bamiro OA, Bakre LG, Alabi A, Ashidi JS, *et al.* Ethnomedicinal herbs in African traditional medicine with potential activity for the prevention, treatment, and management of coronavirus disease 2019. *Fut J Pharm Sci*. 2021 Dec;7:1–4.
- Sun W, Shahrajabian MH, Cheng Q. Fenugreek cultivation with emphasis on historical aspects and its uses in traditional medicine and modern pharmaceutical science. *Mini Rev Med Chem*. 2021 May 1;21(6):724–30.
- Pradeep M, Kruszka D, Kachlicki P, Mondal D, Franklin G. Uncovering the phytochemical basis and the mechanism of plant extract-mediated eco-friendly synthesis of silver nanoparticles using ultra-performance liquid chromatography coupled with a photodiode array and high-resolution mass spectrometry. *ACS Sustain Chem Eng*. 2021 Dec 16;10(1):562–71.
- Bose S, Malik J, Mandal SC. Application of phytochemicals in pharmaceuticals. In: *Advances in pharmaceutical biotechnology: recent progress and future applications*. Singapore, Springer Nature; 2020. pp. 55–68.
- Jeevanandam J, Aing YS, Chan YS, Pan S, Danquah MK. Nanoformulation and application of phytochemicals as antimicrobial agents. In *Antimicrobial nanoarchitectonics*. Elsevier; 2017. pp. 61–82.
- Tripoli E, La Guardia M, Giammanco S, Di Majo D, Giammanco M. Citrus flavonoids: molecular structure, biological activity and nutritional properties: a review. *Food Chem*. 2007 Jan 1;104(2):466–79.
- Lam TP, Tran NV, Pham LH, Lai NV, Dang BT, Truong NL, *et al.* Flavonoids as dual-target inhibitors against  $\alpha$ -glucosidase and  $\alpha$ -amylase: a systematic review of *in vitro* studies. *Nat Prod Bioprospecting*. 2024;14(1):4.
- Chakraborty SB, Hancz C. Application of phytochemicals as immunostimulant, antipathogenic and antistress agents in finfish culture. *Rev Aquaculture*. 2011;3(3):103–19.
- Chakraborty SB, Horn P, Hancz C. Application of phytochemicals as growth-promoters and endocrine modulators in fish culture. *Rev Aquaculture*. 2014;6(1):1–9.
- Le Ouay B, Stellacci F. Antibacterial activity of silver nanoparticles: a surface science insight. *Nano Today*. 2015;10(3):339–54.
- McShan D, Ray PC, Yu H. Molecular toxicity mechanism of nanosilver. *J Food Drug Anal*. 2014;22(1):116–27.
- De M, Ghosh PS, Rotello VM. Applications of nanoparticles in biology. *Adv Mat*. 2008;20(22):4225–41.
- Salata OV. Applications of nanoparticles in biology and medicine. *J Nanobiotechnol*. 2004 Dec;2:1–6.
- Khan MA, Raza A, Ovais M, Sohail MF, Ali S. Current state and prospects of nano-delivery systems for sorafenib. *Int J Polym Mater Polym Biomat*. 2018 Dec 12;67(18):1105–15.
- Kasithevar M, Saravanan M, Prakash P, Kumar H, Ovais M, Barabadi H, *et al.* Green synthesis of silver nanoparticles using *Alysicarpus monilifer* leaf extract and its antibacterial activity against MRSA and CoNS isolates in HIV patients. *J Interdiscip Nanomed*. 2017 Jun;2(2):131–41.
- Khalil AT, Ovais M, Ullah I, Ali M, Shinwari ZK, Maaza M. Biosynthesis of iron oxide (Fe<sub>2</sub>O<sub>3</sub>) nanoparticles via aqueous extracts of *Sageretia thea* (Osbeck.) and their pharmacognostic properties. *Green Chem Lett Rev*. 2017;10(4):186–201.
- Ovais M, Khalil AT, Islam NU, Ahmad I, Ayaz M, Saravanan M, *et al.* Role of plant phytochemicals and microbial enzymes in biosynthesis of metallic nanoparticles. *Appl Microbiol Biotechnol*. 2018;102:6799–814.
- Ovais M, Khalil AT, Raza A, Islam NU, Ayaz M, Saravanan M, *et al.* Multifunctional theranostic applications of biocompatible green-synthesized colloidal nanoparticles. *Appl Microbiol Biotechnol*. 2018;102:4393–408.
- Salarbashi D, Tafaghodi M, Fathi M, Aboutorabzade SM, Sabbagh F. Development of curcumin-loaded *Prunus armeniaca* gum nanoparticles: synthesis, characterization, control release behavior, and evaluation of anticancer and antimicrobial properties. *Food Sci Nutr*. 2021;9(11):6109–19.

33. Hevener KE, Zhao W, Ball DM, Babaoglu K, Qi J, White SW, *et al.* Validation of molecular docking programs for virtual screening against dihydropteroate synthase. *J Chem Inform Modeling.* 2009;49(2):444–60.
34. Innocenti A, Firnges MA, Antel J, Wurl M, Scozzafava A, Supuran CT. Carbonic anhydrase inhibitors: inhibition of the membrane-bound human isozyme IV with anions. *Bioorgan Med Chem Lett.* 2004;14(23):5769–73.
35. Zimmerman S, Innocenti A, Casini A, Ferry JG, Scozzafava A, Supuran CT. Carbonic anhydrase inhibitors. Inhibition of the prokaryotic beta and gamma-class enzymes from Archaea with sulfonamides. *Bioorgan Med Chem Lett.* 2004;14(24):6001–6.
36. Jini D, Sharmila S, Anitha A, Pandian M, Rajapaksha RM. *In vitro* and *in silico* studies of silver nanoparticles (AgNPs) from *Allium sativum* against diabetes. *Sci Rep.* 2022 Dec 21;12(1):22109.

**How to cite this article:**

Sil M, Deb D, Dalui S, Chakraborty S, Goswami A, Polikarpov I. *In silico* and *in vitro* evaluation of nano-enhanced therapeutics for diabetes management. *J Appl Pharm Sci.* 2025;15(07):169–178. DOI: 10.7324/JAPS.2025.2411476